






PAPER

Realistic conversion of single-mode squeezed vacuum state to large-amplitude high-fidelity Schrödinger cat states by inefficient photon number resolving detection

RECEIVED
11 May 2022REVISED
9 September 2022ACCEPTED FOR PUBLICATION
27 September 2022PUBLISHED
11 October 2022Dmitry A Kuts^{1,2} , Mikhail S Podoshvedov^{1,2,3}, Ba An Nguyen^{4,5}  and Sergey A Podoshvedov^{1,2} ¹ Laboratory of Quantum Light Engineering, South Ural State University (SUSU), Lenin Av. 76, Chelyabinsk, Russia² Laboratory of Quantum Information Processing and Quantum Computing, South Ural State University (SUSU), Lenin Av. 76, Chelyabinsk, Russia³ Institute of Physics, Kazan Federal University (KFU), 16a Kremlyovskaya St., Kazan, Russia⁴ Thang Long Institute of Mathematics and Applied Sciences (TIMAS), Thang Long University, Nghiem Xuan Yem, Hoang Mai, Hanoi, Vietnam⁵ Institute of Physics, Vietnam Academy of Science and Technology (VAST), 18 Hoang Quoc Viet, Cau Giay, Hanoi, VietnamE-mail: kuts.phys@gmail.com**Keywords:** Schrödinger cat state, photon number resolving detection, single-mode squeezed vacuum state, continuous-variable quantum computing

Abstract

We theoretically propose an efficient way to generate optical analogs of both even and odd Schrödinger cat states (SCSs) of large amplitude with high fidelity and reasonable generation rate. The resources consumed are a single-mode squeezed vacuum state (SMSV) and possibly a single photon or nothing. We report the generation of even (odd) SCS with amplitude 4.2, fidelity higher than 0.99 with success probability a little more than 10^{-7} by subtraction of 30(31) photons from SMSV by ideal photon number detection. In order to reduce the requirements for the sensitivity of photon number resolving (PNR) detector, we show the implementation of even/odd SCSs with the same characteristics with two PNR detectors resolving only 15 photons each instead of 30. In the case of inefficient detector, SCS's size and its fidelity can be kept close to perfect by using highly transmitting beam splitter, but at the cost of very dramatic reduction of the success probability. In order to have certain harmony between the characteristics (large amplitude, high fidelity and acceptable success probability) in the case of imperfect detection, highly transmitting beam splitters should not be used and number of the subtracted photons must be reduced to 10(11).

1. Introduction

Quantum mechanics involves a number of thought experiments that, in most cases, are used to show its weakness in various interpretations. Schrödinger cat states (SCSs) [1] serve basis for doubts about the lack of a clear boundary between the quantum and everyday classical realm. Realization of such bizarre physical objects is expected to resolve the puzzle, at what degree of macroscopicity, if it exists, the object goes on to be quantum [2, 3]. In optics, the SCS corresponds to a superposition of coherent states $|+\beta\rangle$ and $|-\beta\rangle$ with complex amplitudes $\pm\beta$. Although each of component coherent states is considered to be most classical [4], their superposition corresponding to SCS is nonclassical. The squared absolute value of amplitude of the component coherent state $|\beta|^2$, which is approximately equal to its mean photon number, is treated as size of the associated SCS. In this work, for simplicity, we assume β to be real positive, so the SCS size can be characterized simply by β . In order to recognize an optical SCS macroscopic object, its size must be at least much larger than the quantum uncertainty $1/\sqrt{2}$ of the position observable in the coherent state [5].

In addition to their fundamental importance, the SCSs have high application potentials in teleportation [6–9], quantum metrology [10], quantum computation [11, 12] as well as quantum information processing with hybrid entangled states composed of coherent and photonic states [13–15]. SCSs, also called coherent-state

qubits, can be considered to be practical when the coherent components are nearly orthogonal $\langle -\beta | \beta \rangle \approx 0$ what starts from SCS's size $\beta \geq 2$ [13] that is regarded as a significant experimental achievement. Within this context, a number of schemes for generation of optical large-amplitude SCSs in 'flying' modes are demonstrated [16–20]. However, even in best experiments (see, e.g., [20]), the obtained amplitude $\beta = 1.85$ of the SCS is not sufficient for full use of the states in further quantum processing taking into account the insufficiently high fidelity of the generated states. This is mainly due to the fact that the used experimental methods do not allow restoring photon number distribution of SCSs with amplitude larger than 2 that must be shifted towards higher order number states and centered near the Fock state $|n\rangle$ with $n \sim |\beta|^2$. Fidelity is another important characteristic for SCSs to serve as a potential source. It is desirable that the fidelity of the output state will be as high as possible (ideally ≥ 0.99) in order to be able to efficiently convert coherent states on a balanced beam splitter like $|\beta\rangle_1 |\beta\rangle_2 \rightarrow |\sqrt{2}\beta\rangle_1 |0\rangle_2$ [7, 11–13]. Nearly-deterministic Bell state measurement (BSM) of entangled Schrödinger cat states of large amplitude can be realized in the presence of highly efficient photon number resolving detectors since vacuum contribution (no clicks in both modes) only decreases with increasing amplitude of the coherent qubit. A complete BSM of entangled coherent state allows efficient implementation of the controlled-not gate being the cornerstone of quantum algorithms. Otherwise (i.e., the fidelity of the output state is low), the output photon number distribution may contain unwanted coincidence measurement events and quantum processing with coherent states may become ineffective.

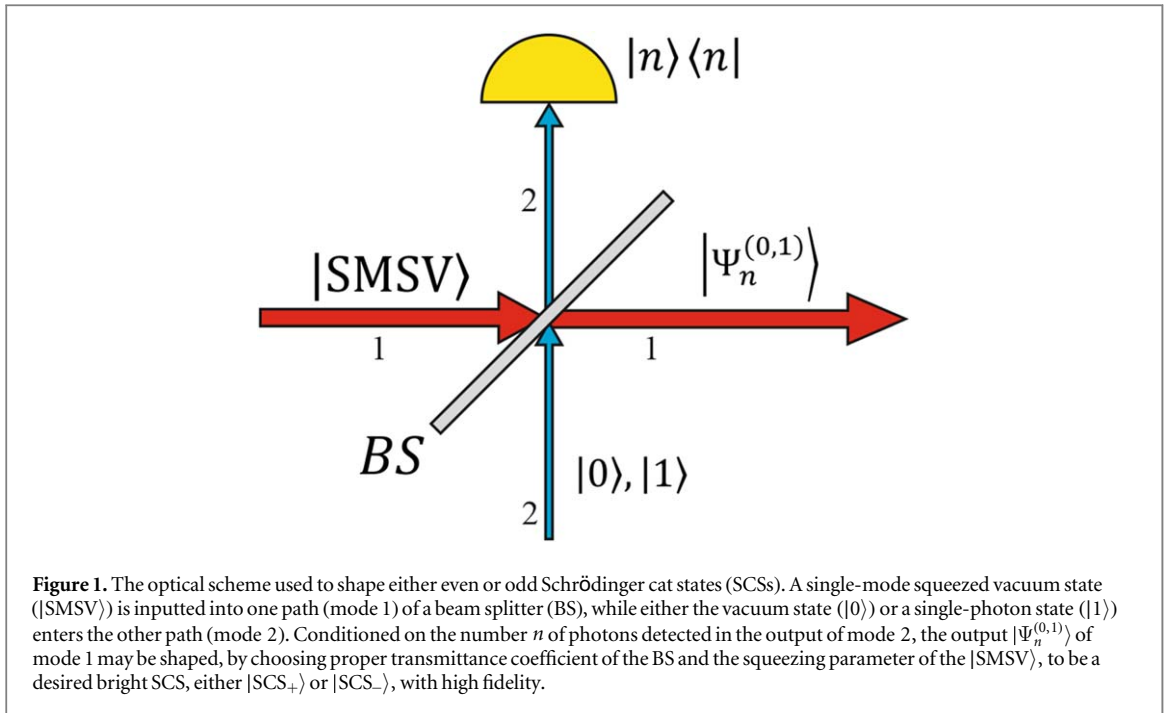
Despite the large number of theoretical proposals for the SCS generation [21–27], implementation of large-amplitude high-fidelity source of event-ready even/odd SCSs has remained a challenging problem even from a theoretical point of view. A standard method for the SCSs generation is photon subtraction [16–27] from the single-mode squeezed vacuum (SMSV) which is a typical nonclassical state containing only even photon numbers (i.e., state with definite, even, parity). In this method, part of the photons resided in the SMSV is diverted to detection channel. The redirection of photons by the beam splitter with a high transmittance coefficient when only a small part of the photons is directed to the measurement mode can significantly reduce the generation rate, which can be defined as $P_{suc} \cdot f_{or}$ with f_{or} being the operating rate of the optical scheme and P_{suc} is the SCSs generation probability. This third important facet of SCS source can take small values, especially, in the case of registration of Fock states with a large number of photons in optical setup with high transmission beam splitter. Therefore, heralded methods need detailed analysis and improvement to brighten its potential in shaping large-amplitude high-fidelity even/odd SCSs generated with a rate sufficiently high for the subsequent continuous-variable (CV) quantum computing.

Here, we give a theoretical analysis of large-amplitude high-fidelity even/odd SCSs source capable to work at high generation rate under ideal conditions. The driving force behind an efficient SCS source is a highly efficient PNR detector [28, 29]. So, we report the generation of large-amplitude high-fidelity even/odd SCSs (say, those with $\beta \simeq 4.2$ which we sometimes call bright cats with fidelity higher than 0.99 and success probability $\sim 10^{-7}$ in scheme with additional input single photon) by extracting a large number of photons (say, either 30 or 31) from the SMSV by ideal PNR detectors with quantum efficiency $\eta = 1$. No restrictions on the beam splitter, being second most important element after PNR detector, are imposed. We consider the possibility of realizing even/odd SCSs with similar characteristics by using two beam splitters and two PNR detectors that could discriminate a smaller (say, 15) number of photons. The parameters of the SCSs generator (amplitude, fidelity, success probability) obtained in the case of using an ideal PNR detector are perfect ones. They are those that should be strived for in the practical case, taking into account the imperfection of the measuring technique. The inefficiency of the detector ($\eta < 1$) can significantly reduce the generation rate, however, leaving the amplitude and fidelity close to perfect if we use a highly transmissive beam splitter. Use of another BS (not highly transmissive one) can increase the success probability (albeit less than perfect), but can significantly reduce the fidelity of the output state. This means that maintaining the three parameters of the SCS source at a level close to perfect is a challenge. To resolve it, we propose the following strategy. To maintain a balance between the three important characteristics ratherish close enough to perfect, we reduce the number of extracted photons (say, to 10 or 11) when dealing with imperfect PNR detectors.

2. SCSs shaping in the case of ideal detection

We begin by describing ingredients to the optical scheme in figure 1. There are two input modes to the beam splitter (BS), labeled mode 1 and mode 2 in the figure. The input state to mode 1 is a single-mode squeezed vacuum (SMSV) state

$$|\text{SMSV}\rangle = \sum_{l=0}^{\infty} b_{2l} |2l\rangle, \quad (1)$$



with amplitudes

$$b_{2l} = \frac{1}{\sqrt{\cosh s}} \left(\frac{\tanh s}{2} \right)^l \frac{\sqrt{(2l)!}}{l!}, \quad (2)$$

where $s > 0$ is the squeezing parameter of the SMSV state, whereas the input state to mode 2 may be either the vacuum state $|0\rangle$ or a single-photon state $|1\rangle$. The SMSV state (1) has a definite parity, which is referred to as even, since it consists exclusively of Fock states with an even number of photons. Another state with definite even parity is the even SCS which has the form (1) but the amplitudes differ. Namely, if we denote the even SCS with amplitude β by $|\text{SCS}_+(\beta)\rangle \equiv |\text{SCS}_+\rangle$, then its full expression reads

$$|\text{SCS}_+\rangle = 2N_+(\beta) \cdot \exp(-\beta^2/2) \sum_{l=0}^{\infty} \frac{\beta^{2l}}{\sqrt{(2l)!}} |2l\rangle, \quad (3)$$

where $N_+ = (2(1 + \exp(-2\beta^2)))^{-1/2}$ is the normalization factor and $\beta > 0$. As an example of the state with definite odd parity, we may mention the so-called odd SCS denoted by $|\text{SCS}_-(\beta)\rangle \equiv |\text{SCS}_-\rangle$ with its full expression as

$$|\text{SCS}_-\rangle = 2N_-(\beta) \cdot \exp(-\beta^2/2) \sum_{l=0}^{\infty} \frac{\beta^{2l+1}}{\sqrt{(2l+1)!}} |2l+1\rangle, \quad (4)$$

with the corresponding normalization factor $N_- = (2(1 - \exp(-2\beta^2)))^{-1/2}$.

If we subtract (add) an even number of photons from (to) the state (1), then it will naturally preserve its parity (i.e., it will remain even), but it will be transformed to a state with a photon number distribution different from that of the initial one. Likewise, subtraction (addition) of an odd number of photons from (to) the SMSV state results in a state with odd parity with totally different photon number distribution. To make use of such properties, let us first consider possible output states of mode 1 in figure 1 when nothing is inputted into mode 2 (formally, it implies that the input state of mode 2 is $|0\rangle$). Then, after the SMSV state passes through a lossless beam splitter BS with $t > 0$ and $r > 0$ the real transmittance and reflectance coefficients transforming creation operators as $a_1^+ \rightarrow ta_1^+ - ra_2^+$, $a_2^+ \rightarrow ra_1^+ + ta_2^+$ and satisfying the physical condition $t^2 + r^2 = 1$, we have [30]

$$\begin{aligned} \widehat{\text{BS}}_{12}(|\text{SMSV}\rangle_1 |0\rangle_2) &= \sum_{l=0}^{\infty} b_{2l} \widehat{\text{BS}}_{12}(|2l\rangle_1 |0\rangle_2) \\ &= \sum_{m=0}^{\infty} \frac{r^{2m}}{\sqrt{(2m)!}} \left(\sum_{k=0}^{\infty} b_{2(k+m)} t^{2k} \sqrt{\frac{(2(k+m))!}{(2k)!}} |2k\rangle_1 \right) |2m\rangle_2 \\ &\quad - \sum_{m=0}^{\infty} \frac{tr^{2m+1}}{\sqrt{(2m+1)!}} \left(\sum_{k=0}^{\infty} b_{2(k+m+1)} t^{2k} \sqrt{\frac{(2(k+m+1))!}{(2k+1)!}} |2k+1\rangle_1 \right) |2m+1\rangle_2. \end{aligned} \quad (5)$$

Depending on the parity of the measurement outcome in the output mode 2, i.e., whether an even or an odd number of photons is detected by PNR detector [28, 29] in figure 1, the output state of mode 1 differs. If the detector finds an even photon number $n = 2m$, then the following conditional state is outputted

$$\begin{aligned} |\Psi_{2m}^{(0)}\rangle &= L_{2m}^{(0)} \sum_{k=0}^{\infty} b_{2(k+m)} t^{2k} \sqrt{\frac{(2(m+k))!}{(2k)!}} |2k\rangle \\ &= \frac{1}{\sqrt{Z^{(2m)}}} \sum_{n=0}^{\infty} y^n \frac{\sqrt{(2(n+m))!}}{(n+m)!} \sqrt{(2n+1)(2n+2)\dots 2(n+m)} |2n\rangle, \end{aligned} \quad (6)$$

where the normalization factor $L_{2m}^{(0)}$ is derived to become $L_{2m}^{(0)} = \sqrt{\cosh s} t^{2m}/y^m \sqrt{Z^{(2m)}}$, $Z^{(m)} = d^{2m}Z/dy^{2m}$ with $Z \equiv Z(y) = Z^{(0)} = 1/\sqrt{1-4y^2}$ and $y = t^2 \tanh s/2$. By definition, the parameter y can take values in the range $0 \leq y \leq 0.5$ in the case of $s > 0$. The limiting values of the parameter y can be taken in the case of either $s = 0$ or $t = 0$ ($y = 0$) which is not of interest and in the case of $t = 1$ and $s \rightarrow \infty$ ($y = 0.5$) going beyond the scope of physical consideration. The success probability to generate the state (6) is

$$P_{2m}^{(0)} = \frac{(1-t^2)^{2m}}{(2m)!L_{2m}^2} = \frac{1}{\cosh s} \left(\frac{1-t^2}{t^2} \right)^{2m} \frac{y^{2m}}{(2m)!} Z^{(2m)} \quad (7)$$

with the superindex '(0)' indicating the case when the input mode 2 is the vacuum state $|0\rangle$. Otherwise, if an odd photon number $n = 2m + 1$ is found, then the output state of mode 1 reads

$$\begin{aligned} |\Psi_{2m+1}^{(0)}\rangle &= L_{2m+1}^{(0)} \sum_{k=0}^{\infty} b_{2(k+m+1)} t^{2k} \sqrt{\frac{(2(m+k+1))!}{(2k+1)!}} |2k+1\rangle \\ &= \sqrt{\frac{y}{Z^{(2m+1)}}} \sum_{n=0}^{\infty} y^n \frac{(2(n+m+1))!}{(n+m+1)!} \sqrt{(2n+2)(2n+3)\dots 2(n+m+1)} |2n+1\rangle, \end{aligned} \quad (8)$$

with the normalization factor $L_{2m+1}^{(0)} = \sqrt{\cosh s} (t^2)^{m+1}/\sqrt{y^{2m+1}Z^{(2m+1)}}$ and the success probability

$$P_{2m+1}^{(0)} = \frac{t^2(1-t^2)^{(2m+1)}}{(2m+1)!L_{2m+1}^2} = \frac{1}{\cosh s} \left(\frac{1-t^2}{t^2} \right)^{2m+1} \frac{y^{2m+1}}{(2m+1)!} Z^{(2m+1)}. \quad (9)$$

The physical condition $\sum_{m=0}^{\infty} (P_{2m}^{(0)} + P_{2m+1}^{(0)}) = 1$ is guaranteed as can be directly checked. Obviously, the conditional state in equation (6) is even while that in equation (8) is odd. Roundly speaking, the parity of the output state (6) and the original input SMSV state (1) are the same, but their expansion amplitudes (i.e., their photon number distribution) are not. Also for the output state (8), its parity changes compared with that of the original input SMSV state (1) and its distribution in photon numbers is totally different. Moreover, the amplitudes b_{2k} of the original SMSV change to $b_{2(k+m)}$ ($b_{2(k+m+1)}$) due to the redistribution of photons by the BS. The proximity between the output states and the even/odd SCSs is evaluated by the fidelities $F_{2m}^{(0)}(\beta) = |\langle \text{SCS}_+ | \Psi_{2m}^{(0)} \rangle|^2$ and $F_{2m+1}^{(0)}(\beta) = |\langle \text{SCS}_- | \Psi_{2m+1}^{(0)} \rangle|^2$, respectively.

The output states $|\Psi_n^{(0)}\rangle$, with $n = 2m$ or $n = 2m + 1$, depend on the squeezing parameter s of the input squeezed state, the transmittance coefficient t of the BS and the detection outcome n , while the target states $|\text{SCS}_{\pm}\rangle$ depend only on β . So, the fidelities $F_n^{(0)}$ depend on all the parameters s , t , n and β , but the probabilities $P_n^{(0)}$ depend only on s , t and n . We display in figures 2(a) and (b) our numerical simulation for the dependence on β and n of the fidelity maximalized over s and t , i.e., $F_{\max}^{(0)}(\beta, n) = \max_{s,t} F_n^{(0)}(\beta, n, s, t)$. For fixed n and β program calculates the value of the fidelity on the grid chosen and looks for the maximum value of $F_{\max}^{(0)}(\beta, n)$. Such maximum values of the fidelity appear as a smooth curve with the following behaviors: for a given n the maximalized fidelity decreases with increasing β and for a given β it increases with increasing n . Generally, an arbitrarily high value of the fidelity with a desired value of β can be obtained if n is large enough. For example, as seen from figures 2(a) and (b), a fidelity greater than or equal to 0.99 for $\beta \geq 2$ is achievable for $n \geq 10$. Subtraction of smaller numbers of photon would lead to the generation of the even/odd SCSs state of amplitude $\beta < 2$ [16–20]. It is also observed that for a given n there is a value of amplitude $\beta_{0.99}^{(0)}(n)$ such that the maximized fidelity is higher than 0.99 for $\beta < \beta_{0.99}^{(0)}(n)$ but falls down rather quickly for $\beta \geq \beta_{0.99}^{(0)}(n)$. The value of $\beta_{0.99}^{(0)}(n)$ itself grows with increasing n : for instance, $\beta_{0.99}^{(0)}(30) = 3.1 > \beta_{0.99}^{(0)}(12) = 2$. Although values of the parameters (s , t) can be determined that make the fidelities maximal, these maximalizing parameters are largely scattered, i.e., they appear very different even with a slight variation in β . This feature leads to a significant spread in the output state's generation probability as shown by colored symbols in figures 2(c) and (d) that correspond to figures 2(a) and (b), respectively. The probability distributions in figures 2(c) and (d) look like structureless swarms.

To get rid of such structureless swarms of success probabilities, we optimize the experimental parameters. Contour lines of the fidelities for the state $|\Psi_{2m}^{(0)}\rangle$ in figure 3(a) clarify the optimization procedure. So, the high fidelities $F_n^{(0)}(\beta, n, s, t) \geq 0.99$ occupy a narrow area (highlighted in blue) stretching from top to bottom on

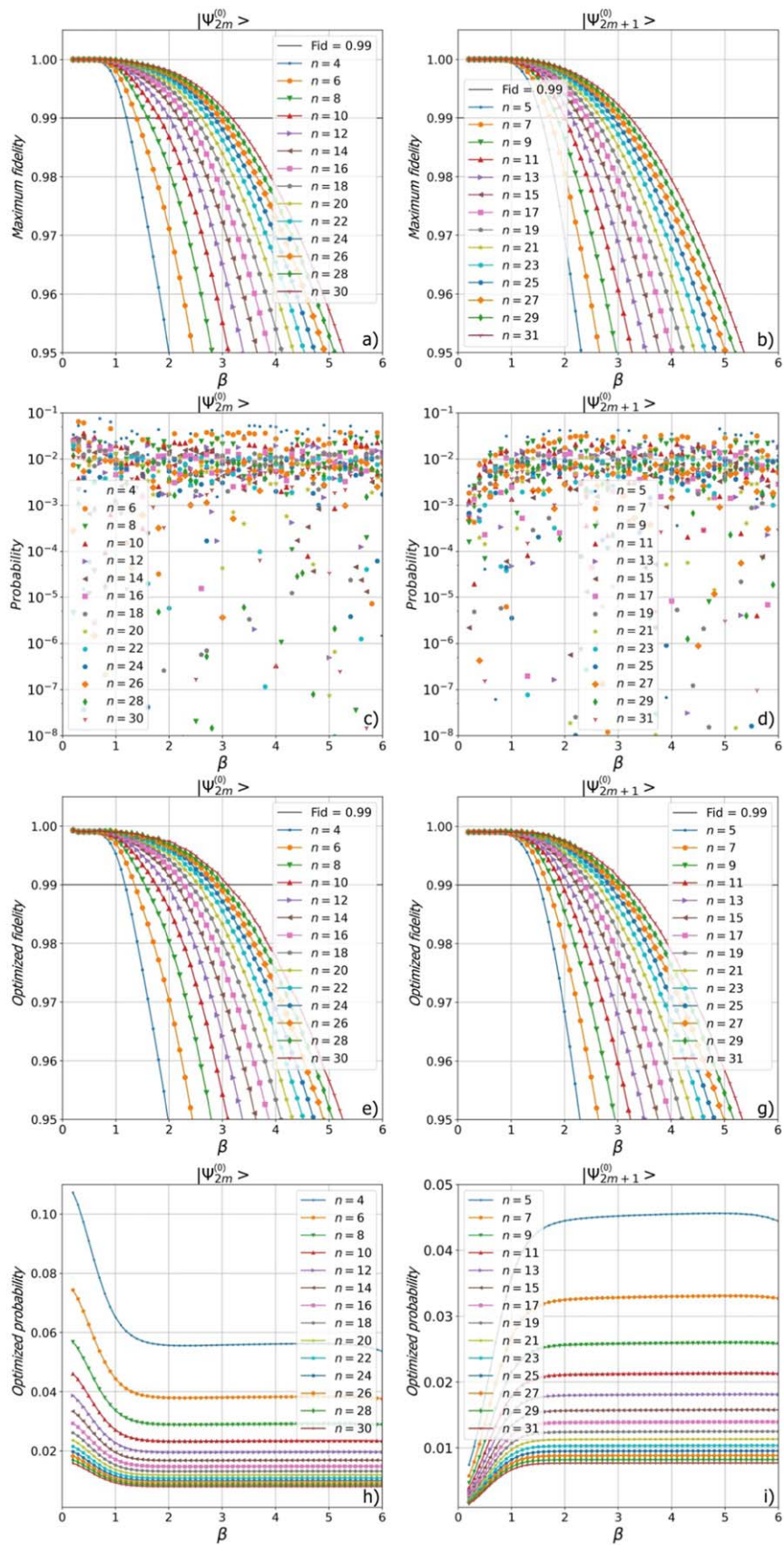


Figure 2. Dependencies of the maximum values of fidelities $F_n^{(0)}$ and corresponding probabilities $P_n^{(0)}$ on β and n when (a), (c) $n = 2m$ and (b), (d) $n = 2m + 1$. In (a), (b) the values of s, t are chosen to maximize the fidelities. With so chosen values of s, t the probabilities are irregularly scattered, as shown in (c), (d). The quantities in (e), (g), (h), (i) are optimized so that the fidelity maintains good enough and the probability becomes highest possible (see text).

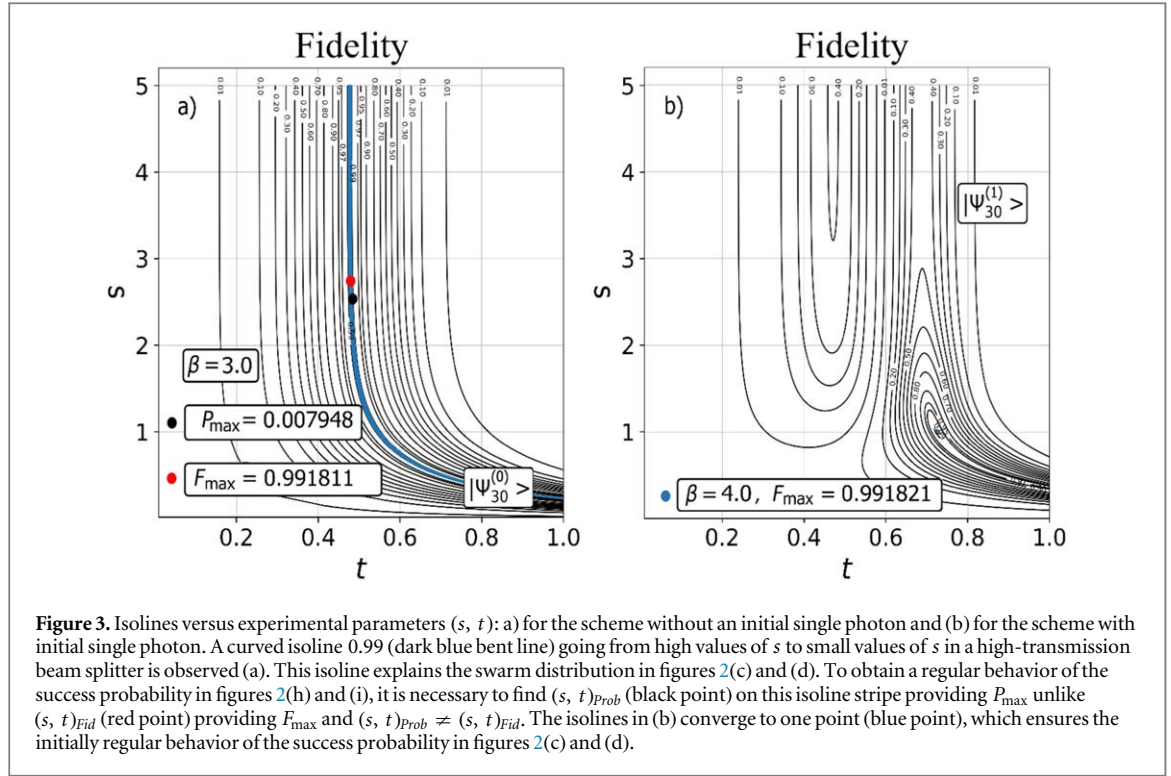


Figure 3. Isolines versus experimental parameters (s, t) : a) for the scheme without an initial single photon and (b) for the scheme with initial single photon. A curved isoline 0.99 (dark blue bent line) going from high values of s to small values of s in a high-transmission beam splitter is observed (a). This isoline explains the swarm distribution in figures 2(c) and (d). To obtain a regular behavior of the success probability in figures 2(h) and (i), it is necessary to find $(s, t)_{Prob}$ (black point) on this isoline stripe providing P_{max} unlike $(s, t)_{Fid}$ (red point) providing F_{max} and $(s, t)_{Prob} \neq (s, t)_{Fid}$. The isolines in (b) converge to one point (blue point), which ensures the initially regular behavior of the success probability in figures 2(c) and (d).

the (s, t) plane. Choosing values of (s, t) from a given curved stripe provides fidelity close to the maximum $F_n^{(0)} \geq 0.99$ but the corresponding probabilities in equation (7) may differ very much. Within this stripe, one can find values of (s, t) denoted by $(s, t)_{Fid}$ that provide the highest possible fidelity shown in figures 2(a) and (b). Yet, within the same stripe one can also find values of (s, t) denoted by $(s, t)_{Prob}$ that provide the maximum success probabilities. These values do not match $(s, t)_{Fid} \neq (s, t)_{Prob}$. Visually, the difference is shown by two dots in figure 3(a): one in red for $(s, t)_{Fid}$ and the other in black for $(s, t)_{Prob}$. Finally, if we are interested only in obtaining maximum fidelities, then we have curves in figures 2(a) and (c). If we are interested in a more practical case with both sufficiently high fidelity and highest possible success probability, then we refer to figures 2(e) and (h). Note that fidelities $F_{2m}^{(0)} \geq 0.99$ are also observed for small values of the squeezing amplitude s in the case of a high-transmission beam splitter (figure 3(a)), which, nevertheless, can sharply reduce the success probability which is not practical. Concerning generation of an odd SCS, analogical curved stripe corresponding to the fidelity $F_{2m+1}^{(0)} \geq 0.99$ is also observed. The plots in figures 2(b) and (d) are made for those $(s, t)_{Fid}$ that provide maximum fidelity, while figures 2(g) and (i) correspond to $(s, t)_{Prob}$ with maximum success probability and fidelity greater than 0.99. The optimization procedure over probability allows one to observe a more regular pattern in figures 2(h) and (i) which exhibit the following properties. For a given β the optimized probability decreases with increasing n no matter n is even or odd. However, the dependence of the optimized probability on β is sensitive to both the value of β itself and the parity of n : when β is small, e.g., $\beta < 2$, it decreases (increases) with increasing β for a given even (odd) n , but when β is large, e.g. $\beta \geq 2$, it saturates to a certain n -dependent value despite of the further increase in β .

In order to achieve a higher fidelity for a larger value of β , consider the case when a single photon is inputted into mode 2 in figure 1. Then, the mixing of the SMSV state and the single photon on the BS results in [30]

$$\begin{aligned}
 \widehat{BS}_{12}(|SMSV\rangle_1|1\rangle_2) &= \widehat{BS}_{12}\left(\sum_{l=0}^{\infty} b_{2l}|2l\rangle_1|1\rangle_2\right) = \sum_{l=0}^{\infty} b_{2l}\widehat{BS}_{12}(|2l\rangle_1|1\rangle_2) \\
 &= r\left(\sum_{k=0}^{\infty} b_{2k}t^{2k}\sqrt{2k+1}|2k+1\rangle_1\right)|0\rangle_2 \\
 &\quad - t^2\sum_{m=1}^{\infty} \frac{r^{2m-1}\sqrt{(2m)!}}{(2m-1)!}\left(\sum_{k=0}^{\infty} b_{2(k+m)}t^{2k}\sqrt{\frac{(2(k+m))!}{(2k+1)!}}\left(1-\frac{2k+1}{2m}\frac{r^2}{t^2}\right)|2k+1\rangle_1\right)|2m\rangle_2 \\
 &\quad + t\sum_{m=0}^{\infty} \frac{r^{2m}\sqrt{(2m+1)!}}{(2m)!}\left(\sum_{k=0}^{\infty} b_{2(k+m)}t^{2k}\sqrt{\frac{(2(k+m))!}{(2k)!}}\left(1-\frac{2k}{2m+1}\frac{r^2}{t^2}\right)|2k\rangle_1\right)|2m+1\rangle_2. \tag{10}
 \end{aligned}$$

Since the parity of a single-photon state is transparently odd, registration of an even number of photons $n = 2m$ in mode 2 outputs in mode 1 a state of odd parity of the form

$$|\Psi_{2m}^{(1)}\rangle = L_{2m}^{(1)} \sum_{k=0}^{\infty} b_{2(k+m)} t^{2k} \sqrt{\frac{(2(k+m))!}{(2k+1)!}} \left(1 - \frac{2k+1}{2m} \frac{r^2}{t^2}\right) |2k+1\rangle, \quad (11)$$

where $L_{2m}^{(1)}$ is the normalization factor, which occurs with the probability

$$P_{2m}^{(1)} = \frac{2mt^4(1-t^2)^{2m-1}}{(2m-1)!L_{2m}^{(1)2}}. \quad (12)$$

with the exception of $n = 0$, while in equation (11) the superindex '(1)' indicates that the single-photon state $|1\rangle$ is inputted into mode 2. Otherwise, if an odd number of photons $n = 2m + 1$ is detected in mode 2, the output state of mode 1 has an even parity of the form

$$|\Psi_{2m+1}^{(1)}\rangle = L_{2m+1}^{(1)} \sum_{k=0}^{\infty} b_{2(k+m)} t^{2k} \sqrt{\frac{(2(k+m))!}{(2k)!}} \left(1 - \frac{2k}{2m+1} \frac{r^2}{t^2}\right) |2k\rangle, \quad (13)$$

with $L_{2m+1}^{(1)}$ the corresponding normalization factor and the probability of this event is

$$P_{2m+1}^{(1)} = \frac{(2m+1)t^2(1-t^2)^{2m}}{(2m)!L_{2m+1}^{(1)2}}. \quad (14)$$

Of course, $\sum_{m=0}^{\infty} (P_{2m}^{(1)} + P_{2m+1}^{(1)}) = 1$ as should be. The proximity of the output states (11) and (13) to the odd (4) and even (3) SCSs, respectively, is characterized by the fidelity $F_{2m}^{(1)} = |\langle \text{SCS}_- | \Psi_{2m}^{(1)} \rangle|^2$ and $F_{2m+1}^{(1)} = |\langle \text{SCS}_+ | \Psi_{2m+1}^{(1)} \rangle|^2$, respectively, which is completely determined by the set of experimental initial parameters (s , t), the size β of the target SCS and the measurement outcome $n \in \{2m, 2m+1\}$. We numerically plot the dependences of maximum values of the fidelities $F_{2m+1}^{(1)}(\beta)$ and $F_{2m}^{(1)}(\beta)$ in figures 4(a) and (b), respectively. Similar to figures 2(a) and (b), both $F_{2m+1}^{(1)}(\beta)$ and $F_{2m}^{(1)}(\beta)$ increase with the detected number of photons for a given β , but decrease with increasing β for a given measurement outcome $n \in \{2m, 2m+1\}$. It is noticed here that the value of amplitude $\beta_{0.99}^{(1)}(n)$ from which the maximized fidelity starts to fall down below 0.99 is larger than the corresponding value $\beta_{0.99}^{(0)}(n)$ in the case when the vacuum state $|0\rangle$ is inputted into mode 2. For example, from figures 4(a) and (b) in comparison with figures 2(a) and (b), one sees that $\beta_{0.99}^{(1)}(31) \simeq 4.2 > \beta_{0.99}^{(0)}(31) \simeq 3.2$ and $\beta_{0.99}^{(1)}(30) \simeq 4.1 > \beta_{0.99}^{(0)}(30) \simeq 3.1$. This means that the use of a single photon as an input to mode 2 can generate, with high enough fidelity, SCSs of bigger size (i.e., larger value of β) compared to the case of inputting the vacuum to mode 2. It is also interesting to note that in contrast to the previous consideration with the vacuum state inputted into mode 2, now the probabilities $P_{2m+1}^{(1)}(\beta)$ and $P_{2m}^{(1)}(\beta)$ show up as smooth functions of β for each given outcome $n \in \{2m, 2m+1\}$ without any optimization procedure, as seen in figures 4(c) or (d), respectively. In part, this is due to the fact that the fidelities gradually converge to one point of maximal fidelity as shown in figure 3(b) (i.e., there is no long stripe of the fidelities ≥ 0.99). Yet, the dependence of the probabilities $P_n^{(1)}(\beta)$ on β and n is opposite to that of the fidelities $F_n^{(1)}(\beta)$. Namely, as it follows from figures 4(a)–(d), $F_n^{(1)}(\beta)$ increase but $P_n^{(1)}(\beta)$ decrease with increasing n for a given β , while $F_n^{(1)}(\beta)$ decrease but $P_n^{(1)}(\beta)$ increase with increasing β for a given n . The plots in figures 4(e), (g), (h) and (i) show the dependence of s , t on β which provide the fidelity maximum and corresponding success probabilities. So, the plots in figures 4(e) and (h) display values of the parameters s and t under which the plots in figures 4(a) and 4(c) are obtained. The plots in figures 4(g) and (i) show values of the parameters s and t under which the plots in figures 4(b) and (d) are constructed. There are domains of β in which the parameter s (t) changes in an abrupt manner as visual from figure 4(h) (figure 4(i)) which is due to the fact that the maximum value of fidelity disappears in one range of values (s , t) and appears in another. Another explanation maybe as follows: it may be due to a large step of varying β . The fact is that the calculations were carried out not at every point of β but only at certain points β_i with some step $\delta\beta$ ($\beta_{i+1} = \beta_i + \delta\beta$), which was reflected in a sharp (not smooth) change in some points of s , t . Finally, why the values s , t can change so dramatically at the points, maybe it is due to action of both reasons: transition to another region and not so small step $\delta\beta$.

Conditioned on the measurement outcomes, the subscripts of the output states amplitudes are shifted forward by either m ($k \rightarrow k+m$) (equations (6), (11), (13)) or $m+1$ ($k \rightarrow k+m+1$) (equation (8)). This displaces the original SMSV distribution (1) towards Fock states with larger photon numbers, finally becoming uniform distribution, that is $b_{2k} > b_{2(k+1)} \forall k$ but $b_{2k} \sim b_{2(k+1)} \approx 0$ for $k \gg 1$. In addition, each of amplitudes $b_{2(k+m)}$ ($b_{2(k+m+1)}$) receives an extra factor that may amplify them. If one chooses the values of (s , t) in an appropriate way, then the photon number distributions of the conditioned state and the target even/odd SCSs can coincide with fidelity ≥ 0.99 despite small discrepancy between generated and target probabilities (see figure 5). The maximum discrepancy in the probabilities d_m , with subscript n indicating on Fock state $|n\rangle$, is $d_{10} = 0.032906$ (top left plot), $d_{11} = 0.031252$ (top right plot), $d_{18} = 0.023296$ (lower left plot) and $d_{17} = 0.05161$ (lower right plot). Discrepancy can affect the fidelity of the transformation of the coherent states

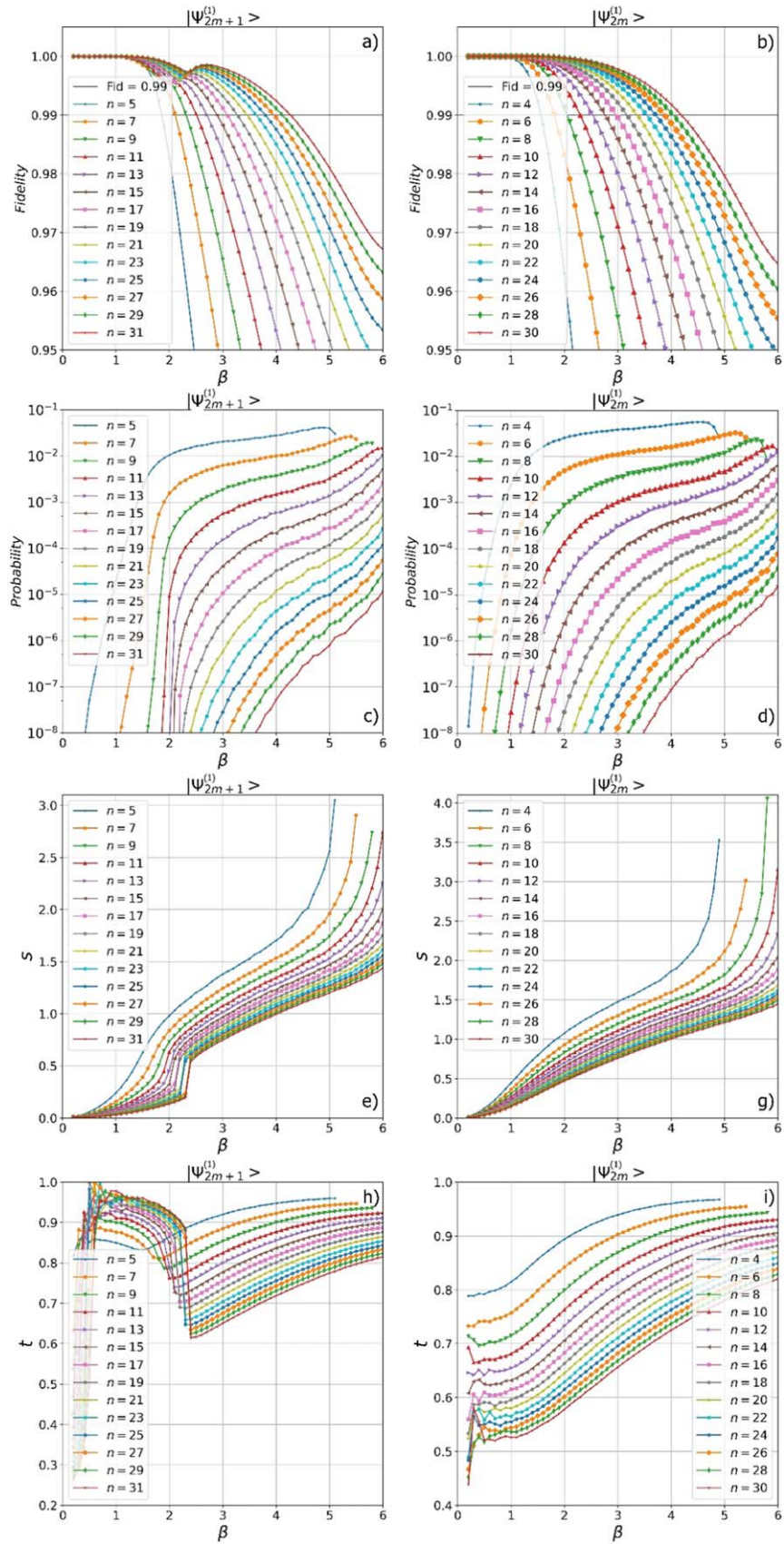
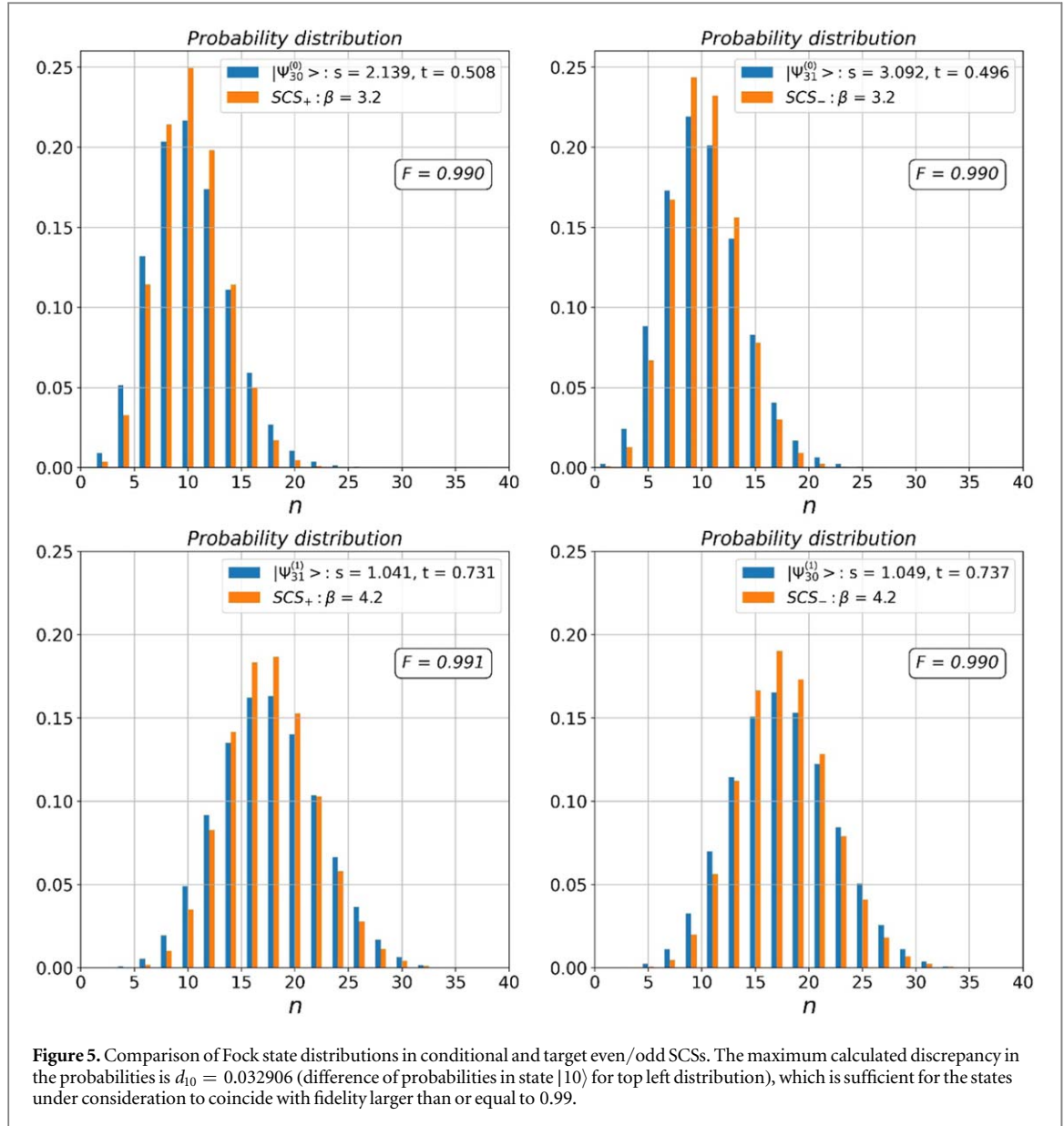


Figure 4. Dependencies of the maximum values of fidelities $F_n^{(1)}$ and corresponding probabilities $P_n^{(1)}$ on β and n when (a), (c) $n = 2m + 1$ and (b), (d) $n = 2m$. The dependences of s (e) and t (h) on β provide the fidelities and probabilities in (a), (c), while the dependences of s (g) and t (i) on β provide the fidelities and probabilities in (b), (d). Sharp changes in s and t (and partly in fidelity) are associated with the transition of the maximum values of the fidelity from one range of parameters (s , t) to another.



on balanced BS: $\widehat{BS}_{12}(|\pm\beta\rangle_1|\pm\beta\rangle_2) = |\pm\sqrt{2}\beta\rangle_1|0\rangle_2$ and $\widehat{BS}_{12}(|\pm\beta\rangle_1|\mp\beta\rangle_2) = |0\rangle_1|\mp\sqrt{2}\beta\rangle_2$, but can be significantly reduced with choice of the experimental parameters providing fidelity very close to 1.

3. Generation of even/odd SCSs by using two PNR detectors

Above, we considered the possibility of creating an even/odd SCS generator by subtracting a number of photons by one PNR detector. The registration of a large number (30, 31) of photons imposes serious requirement on the detector sensitivity, which can be difficult to implement at the current level of technology development. To reduce the requirement for PNR detector to discriminate the number of photons, consider extension of the optical scheme in figure 6, where the original SMSV passes through two beam splitters BS_{12} and BS_{13} with parameters (t_1, r_1) and (t_2, r_2) , respectively. Reflected photons from BS_{12} (second mode) and BS_{13} (third mode) are monitored with two PNR detectors. Then, depending on the number of registered photons by two PND detectors (n, n_1) , the conditioned state $|\Psi_{n,n_1}^{(0,0)}\rangle$ is generated. Using the previously developed approach, we have

$$\widehat{BS}_{13}\widehat{BS}_{12}(|\text{SMSV}\rangle_1|0\rangle_2|0\rangle_3) = \frac{1}{\sqrt{\cosh s}}$$

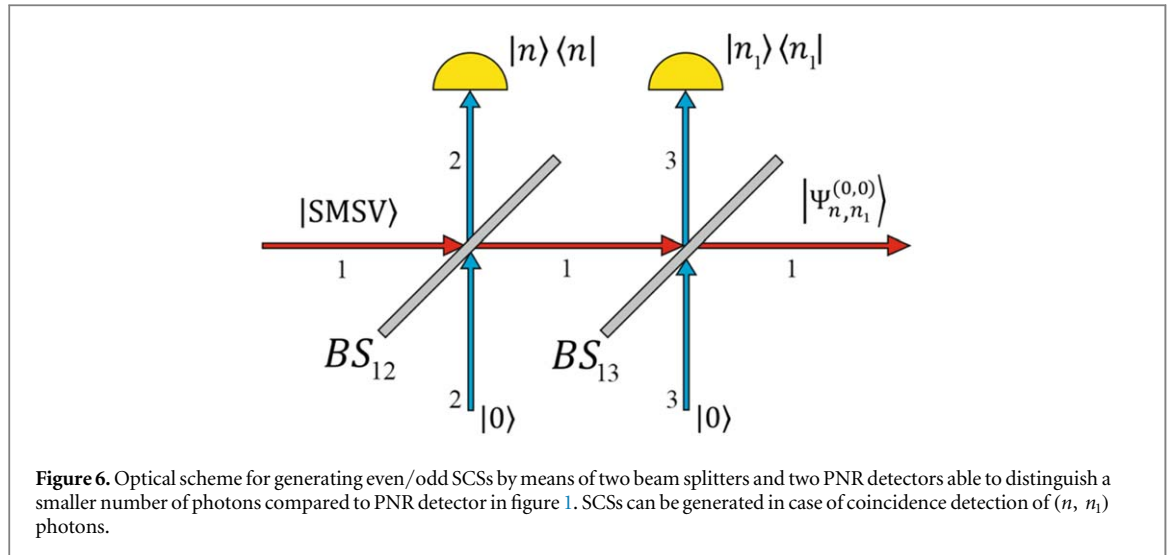


Figure 6. Optical scheme for generating even/odd SCSs by means of two beam splitters and two PNR detectors able to distinguish a smaller number of photons compared to PNR detector in figure 1. SCSs can be generated in case of coincidence detection of (n, n_1) photons.

$$\left(\begin{array}{l} \sum_{m=0}^{\infty} \sum_{m_1}^{\infty} C_{2m,2m_1}^{(0,0)} |\Psi_{2m,2m_1}^{(0,0)}\rangle_1 |2m\rangle_2 |2m_1\rangle_3 \\ - \sum_{m=0}^{\infty} \sum_{m_1}^{\infty} C_{2m,2m_1+1}^{(0,0)} |\Psi_{2m,2m_1+1}^{(0,0)}\rangle_1 |2m\rangle_2 |2m_1+1\rangle_3 \\ - \sum_{m=0}^{\infty} \sum_{m_1}^{\infty} C_{2m+1,2m_1}^{(0,0)} |\Psi_{2m+1,2m_1}^{(0,0)}\rangle_1 |2m+1\rangle_2 |2m_1\rangle_3 \\ + \sum_{m=0}^{\infty} \sum_{m_1}^{\infty} C_{2m+1,2m_1+1}^{(0,0)} |\Psi_{2m+1,2m_1+1}^{(0,0)}\rangle_1 |2m+1\rangle_2 |2m_1+1\rangle_3 \end{array} \right), \quad (15)$$

where amplitudes of the state are the following:

$$\begin{aligned} C_{2m,2m_1}^{(0,0)} &= (r_1/t_1)^{2m} (r_2/t_2)^{2m_1} (y^m y_1^{m_1+1/2} / \sqrt{(2m)!(2m_1)!}) \sqrt{Z^{(2(m+m_1))}(y_1)}, \\ C_{2m,2m_1+1}^{(0,0)} &= (r_1/t_1)^{2m} (r_2/t_2)^{2m_1+1} (y^m y_1^{m_1+1/2} / \sqrt{(2m)!(2m_1+1)!}) \sqrt{Z^{(2(m+m_1)+1)}(y_1)}, \\ C_{2m+1,2m_1}^{(0,0)} &= (r_1/t_1)^{2m+1} (r_2/t_2)^{2m_1} (y^{m+1/2} y_1^{m_1} / \sqrt{(2m+1)!(2m_1)!}) \sqrt{Z^{(2(m+m_1)+1)}(y_1)}, \\ C_{2m+1,2m_1+1}^{(0,0)} &= (r_1/t_1)^{2m+1} (r_2/t_2)^{2m_1+1} (y^{m+1/2} y_1^{m_1+1/2} / \sqrt{(2m+1)!(2m_1+1)!}) \sqrt{Z^{(2(m+m_1)+1)}(y_1)} \end{aligned}$$

and introduced even states become

$$\begin{aligned} |\Psi_{2m,2m_1}^{(0,0)}\rangle &= \frac{\sum_{n=0}^{\infty} y_1^n \frac{\sqrt{(2(n+m+m_1))!}}{(n+m+m_1)!} \sqrt{(2n+1)(2n+2)\dots 2(n+m+m_1)} |2n\rangle}{\sqrt{Z^{(2(m+m_1))}(y_1)}}, \\ |\Psi_{2m+1,2m_1+1}^{(0,0)}\rangle &= \frac{\sum_{n=0}^{\infty} y_1^n \frac{\sqrt{(2(n+m+m_1+1))!}}{(n+m+m_1+1)!} \sqrt{(2n+1)(2n+2)\dots 2(n+m+m_1+1)} |2n\rangle}{\sqrt{Z^{(2(m+m_1+1))}(y_1)}} \end{aligned} \quad (16)$$

and odd CV states

$$\begin{aligned} |\Psi_{2m,2m_1+1}^{(0,0)}\rangle &= |\Psi_{2m+1,2m_1}^{(0,0)}\rangle \\ &= \frac{\sqrt{y_1} \sum_{n=0}^{\infty} y_1^n \frac{\sqrt{(2(n+m+m_1+1))!}}{(n+m+m_1+1)!} \sqrt{(2n+2)(2n+3)\dots 2(n+m+m_1+1)} |2n+1\rangle}{\sqrt{Z^{(2(m+m_1+1))}(y_1)}}, \end{aligned} \quad (17)$$

where $y_1 = y_2^2$. Here, the subscript (n, n_1) indicates the number of detected photons in the second and third auxiliary modes, and the subscript $(0, 0)$ shows that vacuum states are used in input auxiliary modes. Success probabilities to generate the heralded states in equations (16) are the following: $P_{2m,2m_1}^{(0,0)} = |C_{2m,2m_1}^{(0,0)}|^2$, $P_{2m,2m_1+1}^{(0,0)} = |C_{2m,2m_1+1}^{(0,0)}|^2$, $P_{2m+1,2m_1}^{(0,0)} = |C_{2m+1,2m_1}^{(0,0)}|^2$ and $P_{2m+1,2m_1+1}^{(0,0)} = |C_{2m+1,2m_1+1}^{(0,0)}|^2$, respectively. Comparing the states with those in equations (6), one can see that the difference between them is only in different values of the parameters y and y_1 . Despite the difference in the parameters, one can choose values (t_1, t_2, s) that would provide the same fidelity as in figures 2, 4 between the measurement-induced states (16) and even/odd SCSs (equations (3), (4)). The use of two PNR detectors makes it possible to reduce the requirements for the sensitivity of the detectors to recognize the number of incoming photons. For example, if the SCS generator is configured

to implement an even high-amplitude SCS by subtraction of 30 photons, then it can be implemented using the optical setup in figure 6, where each of the PNR detectors measures only 15 photons.

4. Case of imperfect detection

So far we have considered the perfect PNR detection when the quantum efficiency η is 1. In reality, PNR detectors are imperfect whose efficiency, though can be very close to 1, remains less than 1, i.e., $\eta < 1$ [28, 29]. We model the imperfect detector by placing the fictitious beam splitter of transmissivity η before the perfect detector which is responsible for the loss of some of the unregistered photons to derive the positive-operator values measure (POVM) element of the PNR detector with imperfect detection efficiency $\eta < 1$. For example, for $n = 2m$: $\Pi_{2m}(\eta) = \sum_{x=0}^{\infty} C_{2(m+x)}^{2m} \eta^{2m} (1-\eta)^{2x} |2(m+x)\rangle \langle 2(m+x)| + \sum_{x=0}^{\infty} C_{2(m+x)+1}^{2m} \eta^{2m} (1-\eta)^{2x+1} |2(m+x)+1\rangle \langle 2(m+x)+1|$. Finally, we can compute the fidelity between $\rho_{2m}^{(0)} = \text{tr}_2(\rho^{(0)} \Pi_{2m}(\eta))$ being the density matrix, conditioned by measurement of $2m$ photons, where tr_2 stands for trace operation in second mode and $\rho^{(0)} = (\widehat{\text{BS}}_{12}(|\text{SMSV}\rangle_1|0\rangle_2))(\widehat{\text{BS}}_{12}(|\text{SMSV}\rangle_1|0\rangle_2))^+$ is the density matrix of the original SMSV and vacuum transformed by BS, and target even SCS

$$F_{2m}^{(0)} = \text{tr}(\rho_{2m}^{(0)}(|\text{SCS}_+\rangle \langle \text{SCS}_+|)) = \frac{\sum_{x=0}^{\infty} \frac{(1-\eta)^{2x} (1-t^2)^{2x}}{(2x)! L_{2(m+x)}^2} |\langle \text{SCS}_+ | \Psi_{2(m+x)}^{(0)} \rangle|^2}{\sum_{x=0}^{\infty} \frac{(1-\eta)^{2x} (1-t^2)^{2x}}{(2x)! L_{2(m+x)}^2} \left(1 + (1-\eta) \frac{t^2 (1-t^2) L_{2(m+x)}^2}{(2x+1) L_{2(m+x)+1}^2}\right)}. \quad (18)$$

where tr for trace operation in first mode. Using the equation (18), for η such that $1 - \eta \ll 1$, one can decompose the fidelity over PNR detector inefficiency $1 - \eta$: $F_{2m}^{(0)}(\eta) = F_{2m}^{(0)}(\eta = 1)(1 - (1 - \eta)g_{2m,1}^{(0)} + (1 - \eta)^2g_{2m,2}^{(0)} + \dots)$, where $g_{2m,1}^{(0)} = t^2(1-t^2)L_{2m}^2/L_{2m+1}^2$, $g_{2m,2}^{(0)} = (1-t^2)^2L_{2m}^2/2L_{2(m+1)}^2(2t^4L_{2m}^2/L_{2m+1}^2 + |\langle \text{SCS}_+ | \Psi_{2(m+1)}^{(e)} \rangle|^2 / |\langle \text{SCS}_+ | \Psi_{2m}^{(e)} \rangle|^2 - 1)$. Making use of the relation $b_{2(k+m+1)} = \tanh s \sqrt{(k+m+0.5)/(k+m+1)} b_{2(k+m)}$, one can evaluate the ratio $L_{2m}^2/L_{2m+1}^{(e)2} < (\tanh s)^2 (\langle n \rangle + (m+1)^2)$, that enables to construct the lower bound (LB) restricting the fidelity in the case of imperfect photon number detection

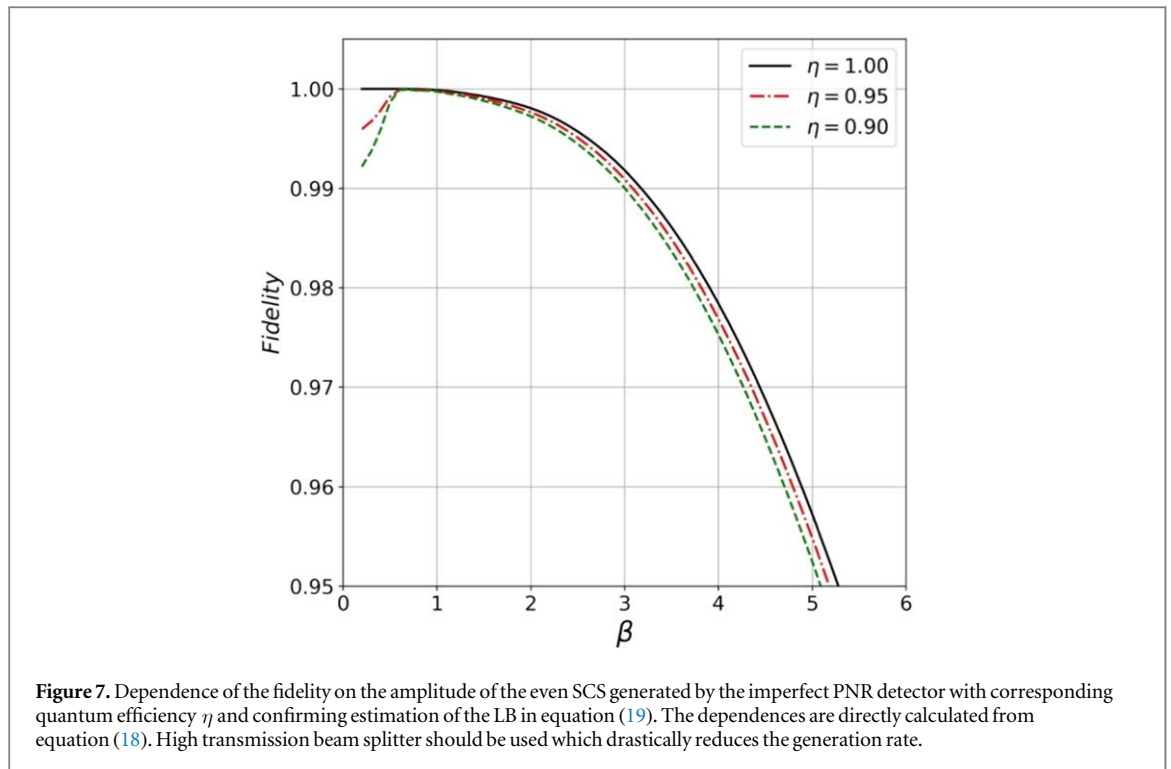
$$F_{2m}^{(0)}(\eta) > F_{2m}^{(0)}(\eta = 1)(1 - (1 - \eta)t^2(1 - t^2)(\tanh s)^2 (\langle n \rangle + (m+1)^2)), \quad (19)$$

with $\langle n \rangle$ the average number of photons in the state $|\Psi_{2m}^{(0)}\rangle$. The inequality (19) is valid in the case of at least $t > 0.4$ to provide $g_{2m,1}^{(0)} \gg g_{2m,2}^{(0)}$, otherwise, the contribution of $g_{2m,2}^{(0)}$ will be comparable with one of $g_{2m,1}^{(0)}$. It should be noted that the range of values $t < 0.4$ is incompatible with the generation of high-amplitude SCS ($\beta \geq 2$) even SCS. Similar expression for the even SCS (3) fidelity can be derived

$$F_{2m+1}^{(1)}(\eta) > F_{2m+1}^{(1)}(\eta = 1) \cdot \left(1 - (1 - \eta)t^2(1 - t^2)(\tanh s)^2 \left(\frac{2(m+1)}{2m+1}\right)^2 (\langle n \rangle + 4m(1+m))\right), \quad (20)$$

where $\langle n \rangle$ is average number of photons in the state $|\Psi_{2m+1}^{(1)}\rangle$ and $g_{2m+1,1}^{(1)} \gg g_{2m+1,2}^{(1)}$ in the case of $t > 0.4$.

There are two strategies for realizing even SCSs by imperfect PNR detection. The first strategy is based on the use of highly transmitting BS, since the LB tends to $F_{2m+1}^{(1)}(\eta = 1)$ in the limit of $t \rightarrow 1$ (figure 7) when only a small fraction of the input photons can be deflected into the measurement mode (visually, this can be explained using figure 3(a) if we trace the curved contour ending at point $t = 1$) and the fidelity of the output state is almost the same as perfect ($F_{2m}^{(0)}(\eta) \cong F_{2m}^{(0)}(\eta = 1)$, $F_{2m+1}^{(1)}(\eta) \cong F_{2m+1}^{(1)}(\eta = 1)$). But a sufficiently high fidelity in figure 7 is accompanied with an extremely low success probability of order of 10^{-18} and even much less, which is far from practical needs. Such generation events become quite rare as the probability to detect n photons has the order r^n . Another strategy does not use highly transmitting BS and is associated with a decrease in the number n of the subtracted photons. It can be more practical, since it also reduces the requirements to PNR detector to distinguish less numbers of photons, for example, 10 or 11 photons instead of 30. To choose such (s, t) one should descend along the bent line into the region of larger values of t and smaller values of s (see figure 3(a)). Graphs confirming the legitimacy of the strategy are shown in figure 8, where the dependences of the success probabilities (on the left side) and corresponding them fidelities (on the right side) on the transmittance t for different values of the quantum efficiencies [29] are shown. The LBs in equations (19), (20) are of one order which leads to approximately similar with those in figure 8 dependences of the success probability and fidelity on the transmittance t . For example, it is possible to realize an even SCS of the amplitude $\beta = 2.5$ with fidelity greater than 0.98 and with success probability about 10^{-11} by extracting 11 photons by PNR with $\eta = 0.98$.



Decomposing the odd fidelities over small parameter $1 - \eta$, one gets *LB*

$$F_{2m+1}^{(0)}(\eta) > F_{2m+1}^{(0)}(\eta = 1) \left(1 - (1 - \eta) \frac{(1 - t^2)}{t^2} \langle n \rangle \right), \quad (21)$$

for the state in equation (8) and

$$F_{2m}^{(1)}(\eta) > F_{2m}^{(1)}(\eta = 1) \left(1 - (1 - \eta) \frac{(1 - t^2)}{t^2} \left(\frac{2m + 1}{2m} \right)^2 \langle n \rangle \right), \quad (22)$$

for the state in equation (11). The inequalities (21) and (22) are valid for $t > 0.4$ to ensure the predominance of contribution of the first order in $(1 - \eta)$ over those of all the higher orders. As in the case of generating even SCS, the range of values $t < 0.4$ does not allow generating odd SCS of larger amplitude ($\beta \geq 2$). The *LB* can take almost zero value in the case of high transmission BS ($t \rightarrow 1$) and $F_{2m+1}^{(0)}(\eta) \cong F_{2m+1}^{(0)}(\eta = 1)$ but such a choice may not be particularly successful as it may lead to a substantial decrease in the success probability as well as a departure from ideal fidelity for odd SCS (see the point of maximum fidelity in figure 3(b)). BS with transmittance $t > 1/\sqrt{2}$ can be in area of interest. Analysis of the data shows that the values of the BS transparency can be chosen in the range $1/\sqrt{2} < t < 0.9$ to provide acceptable generation rate. To keep the fidelity high one can also refuse to extract a large number of photons and limit to smaller number (say 10 or 11) of detected photons by inefficient PNR detector. So, in the case of extracting 11 photons by PNR detector with efficiency $\eta = 0.98$, an odd SCS of amplitude $\beta = 2.5$ with fidelity of about 0.97 and success probability of order 10^{-10} can be generated in a scheme with empty input second mode. Odd SCS of amplitude $\beta = 3$ with fidelity about 0.98 and with success probability of order 10^{-12} can be realized in a scheme with additional single photon by subtracting 10 photons by inefficient PNR detector with quantum efficiency $\eta = 0.98$.

Another factor that can degrade the fidelity of the output state is the presence of the background photons whose mean number of photons in the optical regime at room temperature is approximately 10^{-20} . Influence of the environmental photons and quantum inefficiency of the PNR detector can be modeled by using two fictitious beam splitters, each of which is responsible for the corresponding degrading factor. Photons reflected by the fictitious BS are regarded as photon loss. Thermal state with some mean number of photons can be treated as input in environmental mode. The mathematical consideration of the POVM operators with the two fictitious BS is complex and is beyond the scope of the study. Nevertheless, an estimate of the effect of background photons on the decrease of the fidelity of the output state can be made. Since we use decomposition of the fidelity over small parameter $1 - \eta_{th}$, where η_{th} is a transmittance of ‘thermal’ fictitious BS, comparable to $1 - \eta$, we can note the following. The maximum additional contribution to the fidelity estimate can only come from the outcome with $n - 1$ initial photons and one environmental photon redirected into the measurement mode with a probability proportional to $1 - \eta_{th}$. In the process of the decomposition of the fidelity over parameters $1 - \eta$ and $1 - \eta_{th}$, these two contributions are summed up. The contribution of the

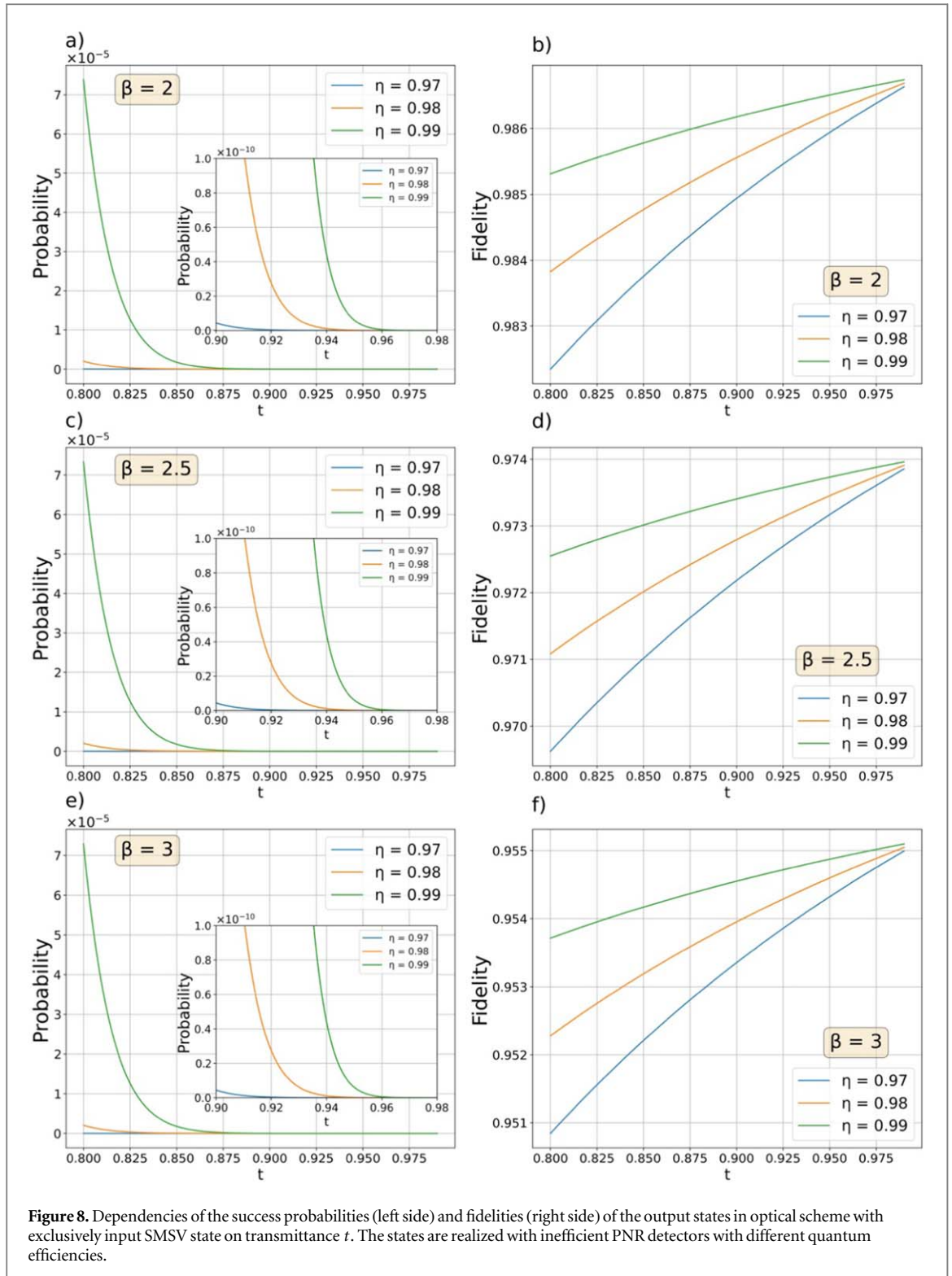


Figure 8. Dependencies of the success probabilities (left side) and fidelities (right side) of the output states in optical scheme with exclusively input SMSV state on transmittance t . The states are realized with inefficient PNR detectors with different quantum efficiencies.

environmental photons, at least, does not exceed one from the action of an inefficient PNR detector. Since the probability of the background photon at the required wavelength is very small, it significantly reduces the contribution of the environmental photon to the amount by which the output fidelity decreases.

5. Discussion

Ability to generate large-amplitude and high-fidelity coherent superpositions is important for scalable continuous-variables quantum computation and quantum information processing but the preparation of the qualitative even/odd SCSs remains a challenging task. We have proposed and analyzed a simple and efficient

way to generate large-amplitude even/odd SCSs with high fidelity and an acceptable for practical use generation rate using irreducible number of the optical elements. Original SMSV state as one of certain parity is used for shaping even/odd SCSs. Using SMSV makes sense since extracting any number of photons in an indistinguishable manner preserves the parity of the output state, leaving output either even or odd. The generation mechanism is based on the redistribution of the photon states by eliminating the contributions of the vacuum and the lower-photon states, which have a larger weight in the initial SMSV distribution and increasing the contribution of the multiphoton states corresponding to $n \sim |\beta|^2$. The mechanism is provided by subtracting a certain number of photons in an indistinguishable manner when information about which initial Fock state of the SMSV contributed to the measurement outcome is lost. Calculations show that SMSV with a squeezing of 5 to 15dB already achievable in experiments can be used. It can also be argued that the use of additional non-Gaussian resource (input single photon) makes it possible to improve such a nonclassical light source by at least two indicators (size of the generated superposition and its fidelity), while leaving the third indicator (generation rate) within the acceptable range. Such generator of the even/odd SCSs with ideal PNR detector ($\eta = 1$) would have perfect values of all three characteristics (size, fidelity and generation rate) and be ready for quantum optical computing [7, 11]. The use of plots in figures 2 and 4 makes it possible to select perfect values for the size, fidelity and the success probability, as well as those input parameters that provide them. So, even/odd SCSs of amplitude $\beta = 4.2$ with fidelity higher than 0.99 can be generated with success probability a little more than 10^{-7} with perfect photon number resolving detection in a scheme with input single photon. If the requirements to the size of the SCS are reduced, say to 3, then the probability of generation with fidelity 0.99 can come close 10^{-4} in the case of subtracting 15 photons in a setup with an input single photon. Note that highest efficiency of spontaneous parametric down conversion (SPDC) is on the order of 1 pair down converted photons per 10^6 pumping photons in waveguides. In the sense, the perfect values of the success probability are comparable and even greater than the probability of generation of down converted photons, which makes it possible to attribute them to reasonable. Such event-ready coherent superposition resource may become ideal for further CV quantum information processing.

The ability of the PNR detector to discriminate large (like either 30 or 31) photon states can be challenge. To reduce the requirements for the PNR detector to resolve large Fock states, an extension of the initial optical setup can be used. It involves two BSs and PNR detectors with a lower sensitivity to the number of measured photons. In the setup in figure 6, generation of target even/odd SCSs is possible in the case of simultaneous registration of a certain number of photons by several PNR detectors. We show that even/odd SCSs can be generated independently of the measured outcomes in figure 6, but the parameters of the experimental setup must be changed from the original version in figure 1. In general, the optical scheme in figure 6 can be extended to a larger number of optical elements (additional BSs, PNR detectors) if one PNR detector is not able to distinguish the required number of photons. The analysis of the quantitative characteristics of an extended optical setup with several PNR detectors requires separate consideration.

Using an imperfect detector with $\eta < 1$ can significantly spoil the perfect values of the SCS source. The resulting expressions for the fidelity allow us to estimate the contribution of various parameters to its decrease. In the case of significant subtraction of the number of photons from original SMSV, say 30 or 31, values of size and fidelity almost sufficiently close to perfect can be achieved in scheme with highly transmissive beam splitter, but at the expense of a sharp decrease in the success probability. The SCSs generation rate can be significantly reduced in order of magnitude by 10^{-18} and even much less since only an insignificant part of the photons can be trapped to measurement mode. To keep all the characteristics at a level somewhat close but nevertheless less perfect, it is required to use beam splitter with transmittance coefficient in a certain range $1/\sqrt{2} < t < 0.9$ and to reduce the number of extracted photons to either 10 or 11 instead of either 30 or 31. Reduction in the number of subtracted photons reduces the values of size and fidelity but allows us to circumvent a drastic decrease of the generation rate thereby maintaining concord between all three characteristics by measurement by inefficient PNR detector. Reducing the number of the subtracted photons makes it possible to achieve an increase in the success probability up to about 10^{-8} for smaller size $\beta < 3$ and fidelity < 0.99 .

In general, subtracting a large number of photons from the SMSV is a promising method for even/odd SCS generation in the presence of a highly efficient PNR detector. The generation rate would be improved by the progress in quality of PNR detection the ability of which to discriminate the number of incoming photons as accurately as possible becomes a decisive factor in the creation of a practical generator of even/odd SCSs of large amplitude. Another possible way to improve the characteristics of the even/odd SCSs generator with input SMSV is related to fragmentation of large Fock state into a smaller number of photons with their subsequent registration by several PNR detectors that requires a separate study. The developed approach can be applicable to other photon states used in auxiliary modes such as arbitrary Fock states, finite superpositions, and even CV states of certain parity. Understanding the issues can give further progress in quantum state engineering of even/odd SCSs.

Acknowledgments

DAK, MSP and SAP are supported by the Ministry of Science and Higher Education of the Russian Federation on the basis of the FSAEIH SUSU (NRU) (Agreement No. 075-15-2022-1116).

Data availability statement

All data that support the findings of this study are included within the article (and any supplementary files).

ORCID iDs

Dmitry A Kuts  <https://orcid.org/0000-0001-6496-443X>

Ba An Nguyen  <https://orcid.org/0000-0002-6802-0388>

Sergey A Podoshvedov  <https://orcid.org/0000-0002-6055-174X>

References

- [1] Schrödinger E 1935 Die gegenwärtige Situation in der Quantenmechanik *Naturwissenschaften* **23** 807–812
- [2] Makus A and Hornberger K 2014 Testing the limits of quantum mechanical superpositions *Nat. Phys.* **10** 271
- [3] Wineland D J 2013 Nobel lecture: superposition, entanglement, and raising Schrödinger's cat *Rev. Mod. Phys.* **85** 1103
- [4] Leonhardt U 2010 *Essential Quantum Optics: From Quantum Measurements to Black Holes* (Cambridge: Cambridge University Press) (<https://doi.org/10.1017/CBO9780511806117>)
- [5] Leggett A J 2002 Testing the limits of quantum mechanics: motivation, state of play, prospects *J. Phys. Condens. Matter* **14** R415
- [6] van Enk S J and Hirota O 2001 Entangled coherent states: teleportation and decoherence *Phys. Rev. A* **64** 022313
- [7] Jeong H and Kim M S 2002 Efficient computation using coherent states *Phys. Rev. A* **65** 042305
- [8] An N B 2003 Teleportation of coherent-state superpositions within a network *Phys. Rev.* **68** 022321
- [9] An N B 2004 Optimal processing of quantum information via type entangled coherent states *Phys. Rev. A* **69** 022315
- [10] Joo J, Munro W J and Spiller T P 2011 Quantum metrology with entangled coherent states *Phys. Rev. Lett.* **107** 083601
- [11] Ralph T C, Gilchrist A, Milburn G J, Munro W J and Glancy S 2003 Quantum computation with optical coherent states *Phys. Rev. A* **68** 042319
- [12] Lund A P, Ralph T C and Haselgrove H L 2007 Fault-tolerant linear optical quantum computing with small-amplitude coherent states *Phys. Rev. Lett.* **100** 030503
- [13] Lee S-W and Jeong H 2013 Near-deterministic quantum teleportation and resource-efficient quantum computation using linear optics and hybrid qubits *Phys. Rev. A* **87** 022326
- [14] Podoshvedov S A 2019 Efficient quantum teleportation of unknown qubit Based on DV-CV Interaction Mechanism *Entropy* **21** 150
- [15] Omkar S, Teo Y S and Jeong H 2020 Resource-efficient topological fault-tolerant quantum computation with hybrid entanglement of light *Phys. Rev. Lett.* **125** 060501
- [16] Ourjoumtsev A, Jeong H, Tualle-Brouiri R and Grangier P 2007 Generation of optical 'Schrödinger cats' from photon number states **448** 784
- [17] Takahashi H et al 2008 Generation of large-amplitude coherent-state superposition via ancilla-assisted photon subtraction *Phys. Rev. Lett.* **101** 233605
- [18] Gerrits T et al 2010 Generation of optical coherent-state superpositions by number-resolved photon subtraction from the squeezed vacuum *Phys. Rev. A* **82** 031802
- [19] Huang K et al 2015 Optical synthesis of large-amplitude squeezed coherent-state superpositions with minimal resources *Phys. Rev. Lett.* **115** 023602
- [20] Sychev D V et al 2017 Enlargement of optical Schrödinger's cat states *Nat. Photonics* **11** 379
- [21] Yurke B and Stoler D 1986 Generating quantum mechanical superpositions of macroscopically distinguishable states via amplitude dispersion *Phys. Rev. Lett.* **57** 13
- [22] Dakna M, Anhut T, Opatrny T, Knöll L and Welsch D G 1997 Generating Schrödinger -cat-like states by means of conditional measurements on a beam splitter *Phys. Rev. A* **55** 3184
- [23] Podoshvedov S A 2012 Schemes for performance of displacing Hadamard gate with coherent states *Opt. Commun.* **285** 3896
- [24] Lund A P, Jeong H, Ralph T C and Kim M S 2004 Conditional production of superpositions of coherent states with inefficient photon detection *Phys. Rev. A* **70** 020101
- [25] Marek P, Jeong H and Kim M S 2008 Generating 'squeezed' superpositions of coherent states using photon addition and subtraction *Phys. Rev. A* **78** 063811
- [26] Podoshvedov S A 2013 Building of one-way Hadamard gate for squeezed coherent states *Phys. Rev. A* **87** 012307
- [27] Mikheev E V, Pugin A S, Kuts D A, Podoshvedov S A and An N B 2019 Efficient production of large-size optical Schrödinger cat states, *Sci. Rep.* **9** 14301
- [28] Lita A E, Miller A J and Nam S W 2008 Counting near-infrared single-photons with 9 % efficiency *Opt. Express* **16** 3032
- [29] Fukuda D et al 2011 Titanium-based transition-edge photon number resolving detector with 98 % detection efficiency with index-matched small-gap fiber coupling *Opt. Express* **19** 870
- [30] Podoshvedov S A and Podoshvedov M S 2021 Entanglement synthesis based on the interference of a single-mode squeezed vacuum and a delocalized photon *JOSA B* **38** 1341